Available online at www.sciencedirect.com
ScienceDirect
Journal of the European Ceramic Society 31 (2011) 2699–2705
www.elsevier.com/locate/jeurceramsoc

High surface area $BaZrO_3$ photocatalyst prepared by base-hot-water treatment

Niki Prastomo [a], Nor Hana binti Zakaria [a], Go Kawamura [b], Hiroyuki Muto [b], Mototsugu Sakai [b], Atsunori Matsuda [b,*]

[a] *Department of Environmental and Life Sciences, Toyohashi University of Technology, Japan*
[b] *Department of Electrical and Electronic Information Engineering, Toyohashi University of Technology, Japan*

Available online 6 April 2011

Abstract

Barium zirconate ($BaZrO_3$) nanoparticles have been prepared by modified sol–gel route. Low temperature process of base-hot-water treatment (BHWT) was conducted to obtain high surface area $BaZrO_3$. The treatments were carried out at 90 °C and at pH 14 with various concentrations of NaOH solution. Single phase nanocrystalline perovskite structure of $BaZrO_3$ powders was successfully obtained by immersing the $BaZrO_3$ precursor into hot-basic condition of 1 M NaOH solution for 1 h and consecutively calcined at 1000 °C for 2 h. $BaZrO_3$ powders with BHWT showed surface area of 18.4 m^2/g which is nearly 8 times larger than those of the powders without BHWT. Photocatalytic activities of $BaZrO_3$ powders upon bleaching of methylene blue in an aqueous solution under UV light irradiation were enhanced by the increment of their surface area.

Keywords: Barium zirconate; Base-hot-water treatment; Photocatalytic activity; Precursors-organic; Powders-chemical preparation

1. Introduction

Barium zirconate ($BaZrO_3$) has been extensively studied and widely used in various applications, such as thermal barrier coating material for aerospace industries. It has distinctive physical and chemical properties such as high thermal stability, excellent chemical durability, low coefficient of thermal expansion, and good structural compatibility.[1–3] Recently, H_2 was produced from pure water with the assist of $BaZrO_3$ photocatalyst upon ultraviolet light irradiation. The highest H_2 evolution rate was up to 522.5 μmol/h g, which was attributed to the calcinated $BaZrO_3$ sample at 1000 °C for 6 h. The surface area of $BaZrO_3$ powders in this case is 5.5 m^2/g.[4] This rate was significantly higher than those attributed by the pure mesoporous anatase TiO_2,[5] Pt(0.3 wt%)–TiO_2(P-25),[6] NiO(3 wt%)–$InTaO_4$,[7] and $NaTaO_3$[8] catalysts. These photocatalytic activities were measured under a similar condition (light source: ∼400 W high-pressure Hg lamps, cell: inner irradiation reaction cells made of quartz, pure water). Therefore, comparison among the photocatalytic activities of these listed catalysts is compatible. High hydrogen production rate of $BaZrO_3$ was ascribed to the highly negative potential of photoinduced electrons, Zr–O–Zr bond angle of 180°, and the large dispersion of its conduction band.[4] It is important that $BaZrO_3$ offered a high photocatalytic activity although surface area of this catalyst was relatively low, i.e. 5.5 m^2/g. Therefore, higher surface area of $BaZrO_3$ powders is presumed to enhance its photocatalytic performance.

In a conventional method based on a solid-state reaction between zirconia and barium carbonate, high temperature treatment is required to synthesize $BaZrO_3$. However, this process produced powders with several undesirable properties, for example, large particle size, wide size distribution, strong agglomeration, and chemical inhomogeneity.[9] Hence, soft chemistry methods gain much more interest from researchers in improving $BaZrO_3$ powder synthesis. In these methods, low temperature decomposition of different precursors was applied to obtain the powder.[9] Various soft chemistry methods in synthesizing $BaZrO_3$ were attempted by different research groups such as thermal decomposition of polymeric precursors,[10–14] combustion mode,[15] coprecipitation reaction,[16] and sol–gel process.[17]

One of the advantages of $BaZrO_3$ powder synthesis via sol–gel process is the production of extremely pure perovskite structure at low crystallization temperatures between 400 and 600 °C.[17] Most of the starting materials for this method are

* Corresponding author. Tel.: +81 532 44 6799; fax: +81 532 48 5833.
E-mail address: matsuda@ee.tut.ac.jp (A. Matsuda).

0955-2219/$ – see front matter © 2011 Elsevier Ltd. All rights reserved.
doi:10.1016/j.jeurceramsoc.2011.03.026

metal alkoxides. However, the use of these metal alkoxides as the starting materials has some setbacks. For example, the numerous kinds of metal alkoxides are difficult to be dealt with due to the high sensitivity towards the atmospheric moisture. Due to the high reactivity of these materials, the rate of alkoxide hydrolysis was difficult to be controlled during the preparation process of multi-component ceramics.[18] The alkoxides are usually expensive as raw materials. Consequently, metal salts are the good alternative starting material for sol–gel process from the viewpoints of chemical stability and cost effectiveness.[18] They can be dissolved in many kinds of organic solvent in which metal complexes are formed. In other words, the metal ions from the metal salts were chelated by organic ligands resulting in the formation of metal complexes. Amines and β-diketones are two of the examples of chelating agents. Metal salts are generally low cost compared with metal alkoxides and the handling of metal salts involved is simpler.

We have reported earlier that base conditions (pH ∼14) of hot-water treatment (BHWT) successfully crystallized sol–gel derived zirconia (ZrO_2) gel powder with high surface area.[19] Chemical structure investigation shows that upon BHWT, the organic moieties were removed and only inorganic component remained. Treatment at pH 14 hot-water with NaOH medium resulted in the formation of tetragonal phase of ZrO_2 with surface area of 292 m^2/g and crystal size of 7 nm.[19] In this work, an attempt to produce high surface area of $BaZrO_3$ which displays high photocatalytic property was conducted by using modified sol–gel process and by applying BHWT. This report describes the effect of chelating agent, BHWT condition, and calcination temperature on the treated samples. In addition, the photocatalytic performance on dye bleaching application of the obtained powders was analyzed. As far as the authors are aware, there have been no papers involving the utilization of $BaZrO_3$ photocatalyst on a dye bleaching application.

2. Experimental procedure

The $BaZrO_3$ sol was prepared from a stoichiometrically 1:1 molar ratio mixture of barium nitrate and zirconium nitrate solutions. Acetylacetonate (AcAc), ethylenediamine-tetraacetate (EDTA), and triethylenetetramine (TETA) were used as chelating agents in this study. Molar ratio of total metal ions to the chelating agent was 1:1. Aging process at 60 °C for 72 h was conducted to obtain $BaZrO_3$ precursors. The acquired $BaZrO_3$ precursor powders were digested by immersing the precursors into hot (90 °C), base-condition water (pH ∼14; 0.5, 1, 1.25, and 1.5 M sodium hydroxide were used as a solution medium) and kept at rest for 1 h without any stirring, followed by washing process by flowing water, thoroughly, and then drying at 60 °C for 12 h. Calcinations at 900, 1000, and 1100 °C for 2 h were then conducted to crystallize the $BaZrO_3$ nanopowders. Untreated samples were also examined for comparison.

Wide-angle X-ray diffraction (XRD) of the $BaZrO_3$ was recorded using a RIGAKU RINT2000. The crystallite size was determined by means of the X-ray line broadening method using the Scherrer equation.[20] Thermal gravimetry (TG) analyses were conducted using a RIGAKU Thermoplus TG8120 under air atmosphere up to 1200 °C with a heating rate of 10 °C/min. Fourier transform infra red (FTIR) spectra of the samples were measured on a JASCO FT/IR-7300 spectrometer in the transmission mode. Standard potassium bromide (KBr) technique was applied. A Hitachi S-4800 field-emission scanning electron microanalyzer (Emax Energy EX-250, Horiba) was used to carry out the energy dispersive spectrometry (EDS) analysis of the products. The morphology of the samples was observed with a transmission electron microscope (TEM, JEOL, JEM-2100F). The specific surface area and the pore volume of the samples was determined by BET and BJH method, respectively, by adsorption/desorption of nitrogen at liquid nitrogen temperature and relative pressures (P/P_0) ranging from 0.1 to 0.25, where P and P_0 are the equilibrium and the saturation pressures of adsorbates at the temperature of adsorption.[18] Before each measurement, the sample was degassed at 300 °C for 30 min. The photocatalytic activities of the samples were evaluated by the degradation of methylene blue (MB) in aqueous solution under the UV light exposure (10 mW/cm^2). Prior to irradiation, the samples were immersed in the MB solution and kept first for 30 min in a dark condition to obtain a stable condition. The remaining concentration of MB upon irradiation was characterized using a UV–visible spectrometer (JASCO, UV-670).

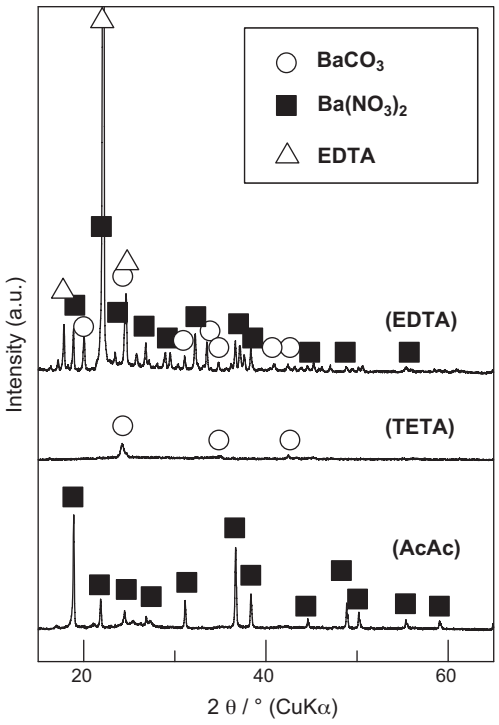

Fig. 1. XRD patterns of as-dried $BaZrO_3$ precursors with various chelating agents. Open circles, closed squares, and open triangles represent diffraction peaks for $BaCO_3$, $Ba(NO_3)_2$, and EDTA crystals respectively.

3. Results and discussion

Fig. 1 shows the XRD patterns of the as-dried $BaZrO_3$ precursors with various chelating agents. In an ideal condition, the chelating agent works as a network builder by reacting with the metal salts. In this case, the chelating agents were expected to

remove the nitrates from the starting materials. However, the utilization of AcAc as a chelating agent failed to remove the nitrates. The crystal form of barium nitrate ($Ba(NO_3)_2$) was observed. In the case of EDTA, mixture of $BaCO_3$, $Ba(NO_3)_2$ and EDTA crystals were found on the precursor. On the other hand, by applying TETA as a chelating agent, the removal of the nitrates was significantly observed, indicating the formation of homogenous metal complexes. However, a small amount of barium carbonate ($BaCO_3$) was obtained. The carbonates were presumably formed due to the reaction with CO_2 in the atmosphere during drying process. Based on this finding, to obtain more homogeneous $BaZrO_3$ precursors, further experiment procedures were conducted using TETA as a chelating agent.

The effect of BHWT on the chemical structure of the as-dried $BaZrO_3$ precursors with TETA is shown in Fig. 2. Amine groups (C–N stretch and N–H bending), carbonates (C=O), alkyl (–C–H), and alcohol (O–H) bands were observed on the as-dried sample. After the BHWT at 90 °C for 1 h under various NaOH concentrations, most of the organic compounds were removed, including amine and carbonates groups. Alkyl group and small amount of carbonate groups were still remaining. By increasing the NaOH concentration during BHWT, no significant differences in terms of chemical structure were detected. This organic compounds removal provides the precursor with porous structure.

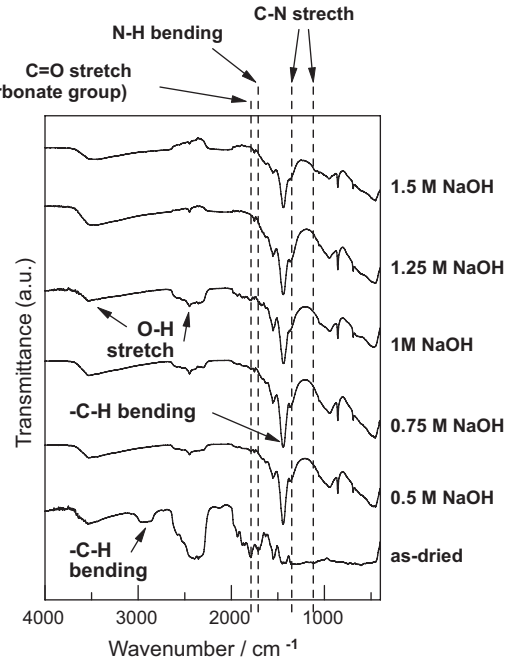

Fig. 2. FTIR spectra of as-dried and BHW-treated $BaZrO_3$ samples. The BHWT was carried out at 90 °C for 1 h with a given NaOH concentration.

The removal of organic compounds on the $BaZrO_3$ samples was also clarified by the thermogravimetry study (Fig. 3a). Smaller weight loss was observed in the BHW-treated samples compared with the as-dried one. At 1200 °C, the as-dried sample contained about 75% burnt compound (organic compound), on the other hand, nearly 25% of the organic compounds were decomposed on the BHW-treated samples. Fig. 3b shows that for the $BaZrO_3$ sample treated with 1 M NaOH, the decomposition of organic compounds ended at around 1000 °C and the weight loss was smallest among the BHW-treated samples.

Fig. 4 shows the XRD patterns of 1 M NaOH as-BHW-treated $BaZrO_3$ sample and after further calcination at 900, 1000, and 1100 °C for 2 h. For the as-treated sample, a crystal structure of $BaCO_3$ was majorly detected. A small amount of tetragonal phase of zirconia (t-ZrO_2) was also observed. As-dried $BaZrO_3$ precursor was formed by chelated structure of metal ions with amine groups of TETA. In addition, EDS measurement showed that no Na^+ ions were detected on all samples. The Na^+ ions content should be too small to be detected by the EDS. The XRD patterns of the calcined samples show that $BaCO_3$ phase still occurred on the $BaZrO_3$ precursor which was calcined at 900 °C. However, by increasing the calcination temperature up to 1000 °C, single phase of $BaZrO_3$ perovskite structure was obtained. Enhancement of $BaZrO_3$ crystallinity,

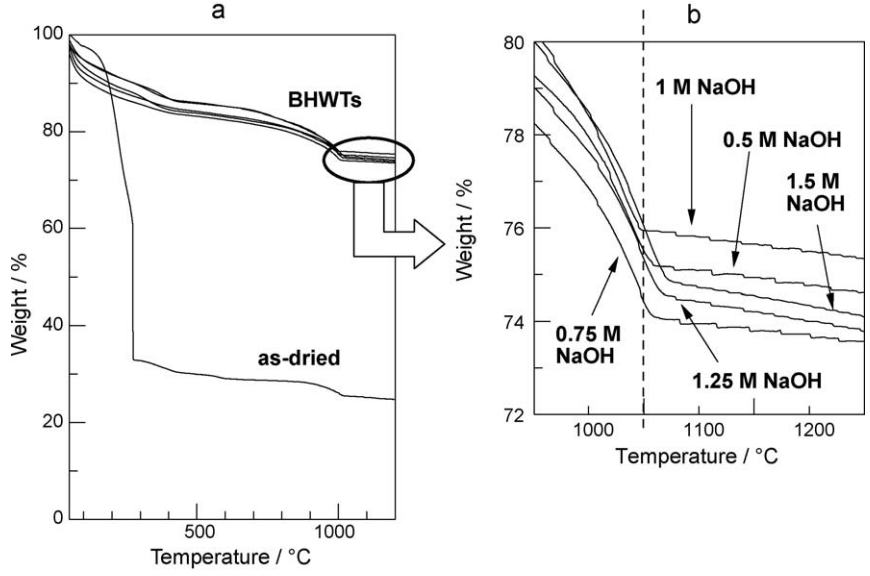

Fig. 3. TG graphs of as-dried and BHW-treated $BaZrO_3$ samples.

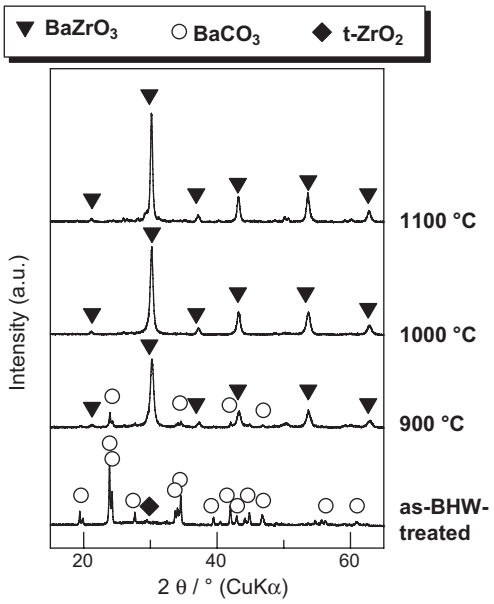

Fig. 4. XRD patterns of BHW-treated BaZrO3 samples before and after calcination at various temperatures. BHWT was carried out at 90 °C for 1 h using 1 M NaOH concentration.

which is shown by the narrow width of the diffraction peaks and the increase in its intensity, was obtained by further increasing the calcination temperature from 1000 to 1100 °C. Compared with the conventional $BaZrO_3$ preparation, based on a solid-state reaction between zirconia and barium carbonate, calcination temperatures at 1350–1400 °C are required to achieve complete formation of $BaZrO_3$.[17] In the soft chemistry process, homogeneous mixing of the reagents at the molecular scale in solution lowers the crystallization temperature of $BaZrO_3$.[4]

Further analysis of the samples was conducted by TEM. Fig. 5 shows the images of 1 M NaOH BHW-treated $BaZrO_3$ sample after further calcination at 900, 1000, and 1100 °C for 2 h. Judging from the TEM data, particle growth of the $BaZrO_3$ was clearly seen. The average particle size for the 900, 1000, and 1100 °C calcined samples were 10, 20, and 35 nm, respectively. Additional study on the effect of NaOH quantity on the particle shape was also carried out. The morphological data of the sample which treated with 0.5, 1, and 1.5 M NaOH then followed with calcination at 1000 °C for 2 h is shown in Fig. 6. Spherical shape with comparable size of the particle was clearly observed from all TEM images. The results show that the quantity of NaOH used during the BHWT did not provide significant effect on the final $BaZrO_3$ particle's morphology.

Fig. 7 shows the Raman spectra of BHW-treated $BaZrO_3$ samples with various concentrations of NaOH after further calcination at 1000 °C for 2 h. A carbonate peak was observed in all samples. However, $BaZrO_3$ sample treated with 1 M NaOH showed smallest amount of carbonates group. These data are in a well agreement with the previous TG analysis of the precursor samples. The removal of organic compounds during BHWT resulted in unpaired-bonds of the Ba^{2+} ions. This condition may provide a chance for the barium unpaired-bonds to react with the atmosphere to produce the carbonates. Lower content of NaOH (0.5 and 0.75 M NaOH) was not successful to completely remove the organic compounds on the precursor. Due to this reason, some of the carbonate groups still remain even after calcination at 1000 °C for 2 h. On the other hand, higher content of NaOH (1.25 and 1.5 M NaOH) was considered to provide extra unpaired-bonds of Ba^{2+} ions upon BHWT, thus, the as-treated precursors become more reactive with the atmosphere and produce more $BaCO_3$ phase.

BHWT was found to be an appropriate process to obtain $BaZrO_3$ powders with small crystal size and high specific surface area (Table 1). Based on XRD and BET data analyses, after calcination at 1000 °C for 2 h, the untreated $BaZrO_3$ sample posses crystal size of 42 nm and specific surface area of 2.4 m^2/g. On the other hand, $BaZrO_3$ powder obtained from BHWT at 90 °C for 1 h using 1 M NaOH has a crystal size of 17 nm with surface area of 18.4 m^2/g, which is nearly 8 times larger than that of the untreated $BaZrO_3$. BJH adsorption and desorption cumulative volume pores values of the samples were found to be ranging from 0.03 to 0.05 cm^3/g. These values of the volume pore could be used to indicate that the sample is still in agglomeration state.

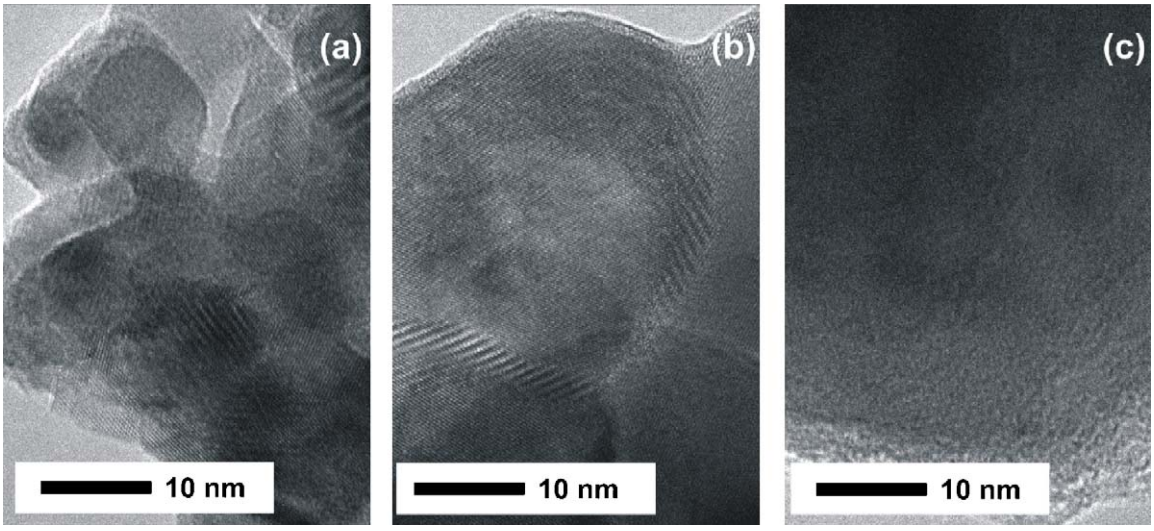

Fig. 5. TEM images of 1 M NaOH BHW-treated $BaZrO_3$ sample after further calcination at (a) 900, (b) 1000, and (c) 1100 °C for 2 h.

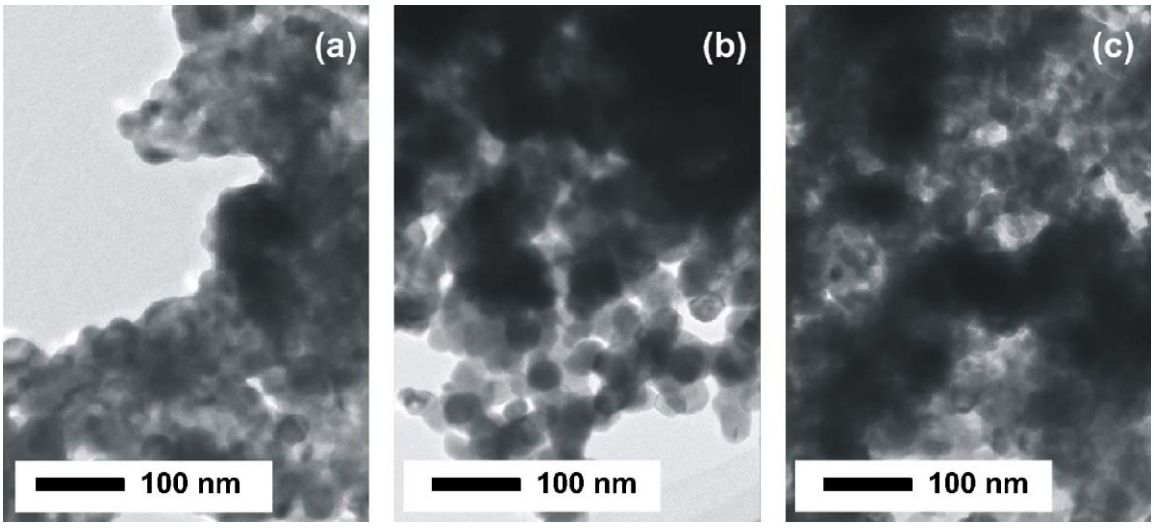

Fig. 6. TEM images of BHW-treated $BaZrO_3$ which treated with (a) 0.5, (b) 1, and (c) 1.5 M NaOH after further calcination at 1000 °C for 2 h.

The agglomerated state was also validated by the TEM images. BHWT at 90 °C for 1 h using 1 M NaOH was found to be optimum in the present conditions to obtain $BaZrO_3$ powder with high surface area with maintaining its small crystal size.

Study on the BHWT time was conducted by analyzing the XRD patterns of the 1 M NaOH–BHW-treated samples for 1, 6, and 12 h and continued with calcination at 1000 °C for 2 h (Fig. 8). Wider and lower intensity of the diffraction peaks was obtained by applying longer BHWT time. This result shows that longer BHWT time suppressed the crystallization of $BaZrO_3$. Further analyses using Scherrer method confirmed the decrease of crystallites size as a function of BHWT time. Crystallite size of $BaZrO_3$ samples of BHW-treated for 1, 6, and 12 h were 17, 15, and 14 nm, respectively. In addition, the increase of BHWT time resulting in the formation of Ba_2ZrO_4 phase. Veith et al.[17] mentioned that the formation of Ba-rich phase Ba_2ZrO_4 was due to the decomposition of undesired $BaCO_3$ by heat treatment. The Ba_2ZrO_4 phase is formed preferably in a $BaCO_3$-rich-condition and might still exist even after the completion of carbonate species decomposition process.[17] Similarly with the high con-

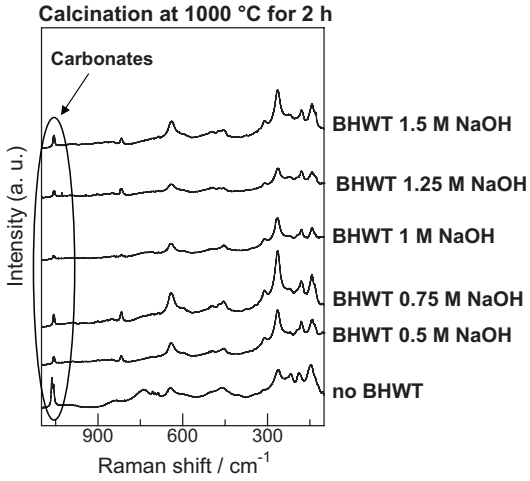

Fig. 7. Raman spectra of BHW-treated $BaZrO_3$ samples with various concentrations of NaOH after further calcination at 1000 °C for 2 h.

Table 1
Crystallite sizes and specific surface area values of BHW-treated and untreated $BaZrO_3$ samples after further heat treatment at 1000 °C for 2 h.

NaOH concentration (M)	$BaZrO_3$ crystal size (nm)[a]	Surface area (m^2/g)[b]
0.5	17	5.4
0.75	17	17.3
1	17	18.4
1.25	18	12.1
1.5	17	4.6
Without BHWT	42	2.4

[a] Derived from XRD data by Scherer method.
[b] Calculated by BET method.

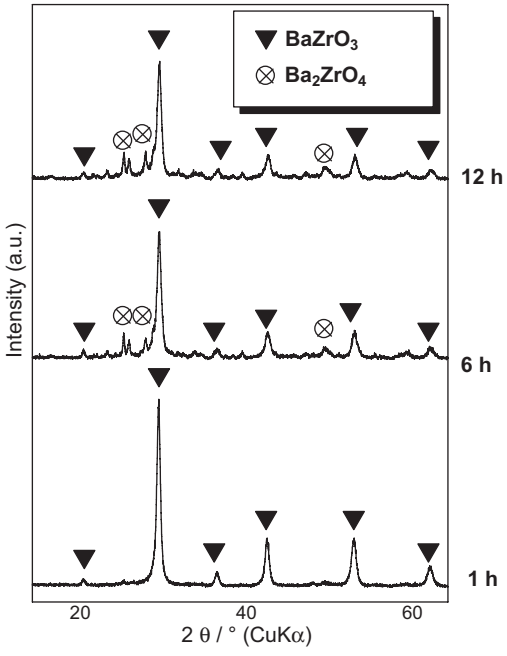

Fig. 8. XRD patterns of 1 M NaOH–BHW-treated $BaZrO_3$ samples for various times and continued by further heat treatment at 1000 °C for 2 h.

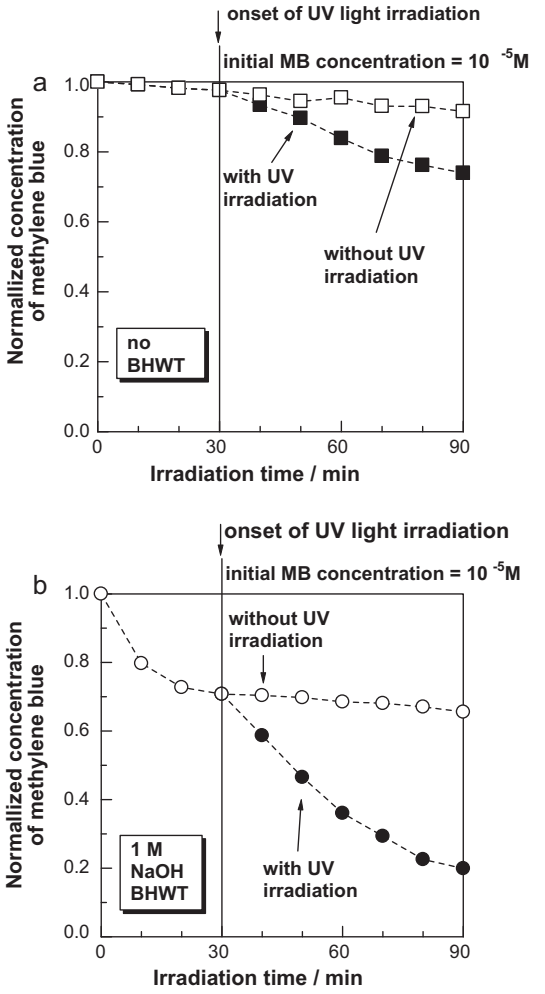

Fig. 9. The photocatalytic degradation of MB in the presence of (a) untreated and (b) BHW-treated $BaZrO_3$ photocatalysts under UV light irradiation.

centration NaOH–BHWT, longer BHWT time also provides more extra unpaired-bonds and results in more atmosphere-reactive precursors. Consequently, more $BaCO_3$ contaminations were produced, thus, the Ba_2ZrO_4 phase was present. In this study, it was found that BHWT time period presents greater consequence on the formation of $BaCO_3$ when compared with the concentration of NaOH on the base-hot-water.

Fig. 9 shows the normalized concentration of MB photocatalitically decomposed by untreated and 1 M NaOH–BHW-treated samples after further calcination at 1000 °C for 2 h. The kinetics plots are shown by apparent first-order linear transform $\ln(C/C_0) = k_{app}t$.[21] The data were shown in Fig. 10. The activity of the photocatalysts was evaluated by comparing the apparent first-order rate constants (k_{app}) and listed in Table 2.

Table 2
Appear rate constants (k_{app}) of MB photodecomposition and linear regression coefficients from a plot of $\ln(C/C_0) = k_{app}t$.

Catalysts	R^2	k_{app} (min^{-1})
No BHWT $BaZrO_3$ without UV irradiation	0.9093	0.001
No BHWT $BaZrO_3$ with UV irradiation	0.988	0.0049
1 M NaOH–BHWT $BaZrO_3$ without UV irradiation	0.9669	0.0013
1 M NaOH–BHWT $BaZrO_3$ with UV irradiation	0.9957	0.0221

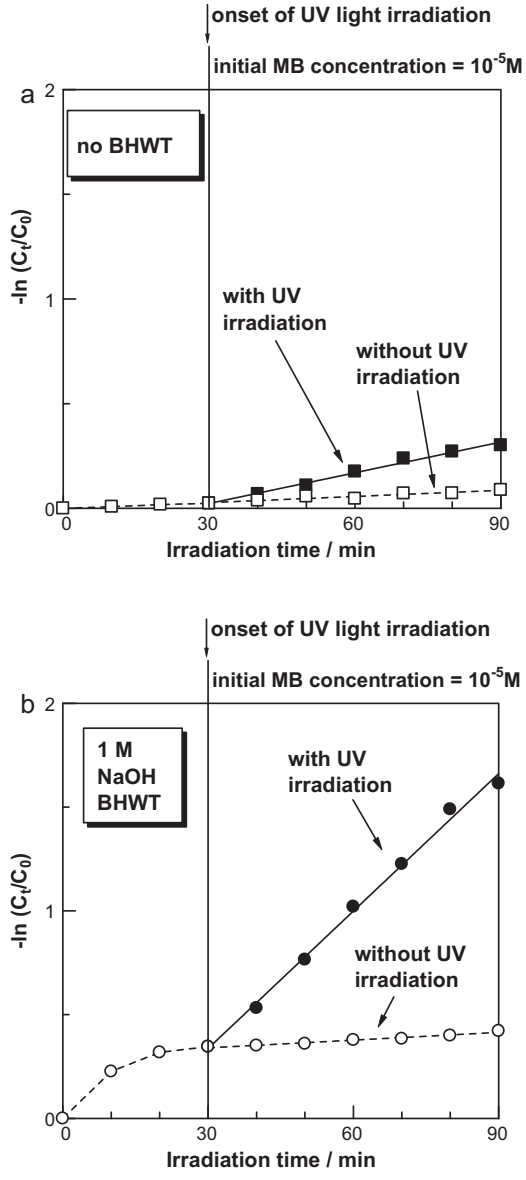

Fig. 10. Apparent first-order linear transforms $\ln(C/C_0)$ of MB degradation kinetic plots for (a) untreated and (b) BHW-treated $BaZrO_3$ photocatalysts under UV light irradiation.

Based on the data from both samples, it is confirmed that $BaZrO_3$ has a photocatalytic activity. Compared with samples without UV irradiation, the amount of MB decomposed was increased by the of UV irradiation. In addition, higher surface area of the BHW-treated $BaZrO_3$ enhances the adsorption of the MB on the surface of the photocatalyst. In the measurement without any UV light irradiation, porous structure of the BHW-treated sample managed to adsorb higher MB concentration from the solution. Moreover, as expected, $BaZrO_3$ powder with higher surface area and purer phase through 1 M

NaOH–BHWT shows enhanced photocatalytic performance (Fig. 9). Untreated and BHW-treated sample under UV light irradiation give apparent rate constants of 0.049 min^{-1} and 0.0221 min^{-1}, respectively (Fig. 10 and Table 2). The utilization of BHWT significantly improved the photocatalytic activity of the resultant $BaZrO_3$ powders.

4. Conclusions

$BaZrO_3$ powder with high surface area was successfully prepared via modified sol–gel process. The usage of TETA as a chelating agent managed to remove the nitrate ligands from the starting materials. As a result, $BaZrO_3$ precursor without any presence of $Ba(NO_3)_2$ crystal was obtained, producing homogeneous precursor of $BaZrO_3$. BHWT was conducted to seek a new technique to acquire $BaZrO_3$ with high surface area. Upon BHWT, the organic compounds from the precursor, including amine groups and carbonate groups, were removed. The organic compounds removal provides a precursor with porous structure. The porous structure was relatively maintained during further calcination at 1000 °C for 2 h. BHW-treated $BaZrO_3$ powder has a specific surface area of 18.4 m^2/g, nearly 8 times larger compared with that of the untreated sample. In addition, photocatalytic study shows that BHW-treated $BaZrO_3$ performed significantly enhanced activity.

Acknowledgements

This work has been partly supported by Japan Society for the Promotion of Science (Grand-in-Aid for Scientific Research (B), No. 20360298). We would like to thank Prof. Noriyoshi Kakuta of Toyohashi University of Technology for the surface area measurements. N.P. acknowledges ASEAN University Network/Southeast Asia Engineering Education Development Network (AUN/SEED-Net) and Japan International Cooperation Agency (JICA) for supporting his PhD study at Toyohashi University of Technology.

References

1. Zhang JL, Evetts JE. $BaZrO_3$ and $BaHfO_3$: preparation, properties and compatibility with $YBa_2Cu_3O_{7-x}$. *J Mater Sci* 1994;**29**:778–85.
2. Erb A, Walker E, Flukiger R. The use of $BaZrO_3$ crucibles in crystal growth of the high-Tc superconductors. Progress in crystal growth as well as in sample quality. *Physica C* 1996;**258**:9–20.
3. Kumar HP, Vijayakumar C, George CN, Solomon S, Jose R, Thomas JK, et al. Characterization and sintering of $BaZrO_3$ nanoparticles synthesized through a single-step combustion process. *J Alloy Compd* 2008;**458**:528–31.
4. Yuan Y, Zhang X, Liu L, Jiang X, Lv J, Li Z, et al. Synthesis and photocatalytic characterization of a new photocatalyst $BaZrO_3$. *Int J Hydrogen Energy* 2008;**33**:5941–6.
5. Jitputti J, Pavasupree S, Suzuki Y, Yoshikawa S. Synthesis and photocatalytic activity for water-splitting reaction of nanocrystalline mesoporous titania prepared by hydrothermal method. *J Solid State Chem* 2007;**180**:1743–9.
6. Arakawa H, Sayama K. Solar hydrogen production. Significant effect of Na_2CO_3 addition on water splitting using simple oxide semiconductor photocatalysts. *Catal Surv Jpn* 2000;**4**:75–80.
7. Chiou Y-C, Kumar U, Wu JCS. Photocatalytic splitting of water on $NiO/InTaO_4$ catalysts prepared by an innovative sol–gel method. *Appl Catal A: Gen* 2009;**357**:73–8.
8. Kudo A. Development of photocatalyst materials for water splitting. *Int J Hydrogen Energy* 2006;**31**:197–202.
9. Bućko MM, Obłąkowski J. Preparation of $BaZrO_3$ nanopowders by spray pyrolysis method. *J Eur Ceram Soc* 2007;**27**:3625–8.
10. Robertz B, Boshini F, Cloots R, Rulmont A. Importance of soft solution processing for advanced $BaZrO_3$ materials. *J Inorg Mater* 2001;**3**:1185–7.
11. Brzezińska-Miecznik J, Haberko K, Bućko MM. Barium zirconate ceramic powder synthesis by the coprecipitation–calcination technique. *Mater Lett* 2002;**56**:273–8.
12. Boschini F, Robertz B, Rulmont A, Cloots R. Preparation of nanosized barium zirconate powder by thermal decomposition of urea in an aqueous solution containing barium and zirconium, and by calcination of the precipitate. *J Eur Ceram Soc* 2003;**23**:3035–42.
13. Hardy A, D'Haen J, Van den Rul H, Van Bael MK, Mullens J. Crystallization of alkaline earth zirconates and niobates from compositionally flexible aqueous solution-gel syntheses. *Mater Res Bull* 2009;**44**:734–40.
14. Magrez A, Schober T. Preparation, sintering, and water incorporation of proton conducting $Ba_{0.99}Zr_{0.8}Y_{0.2}O_{3-\delta}$: comparison between three different synthesis techniques. *Solid State Ionics* 2004;**175**:585–8.
15. Azad A-M, Subramaniam S. Synthesis of $BaZrO_3$ by a solid-state reaction technique using nitrate precursors. *Mater Res Bull* 2002;**37**:85–97.
16. Boschini F, Rulmont A, Cloots R, Vertruyen B. Rapid synthesis of submicron crystalline barium zirconate $BaZrO_3$ by precipitation in aqueous basic solution below 100 °C. *J Eur Ceram Soc* 2009;**29**:1457–62.
17. Veith M, Mathur S, Lecerf N, Huch V, Decker T, Beck HP, et al. Sol–gel synthesis of nano-scaled $BaTiO_3$, $BaZrO_3$ and $BaTi_{0.5}Zr_{0.5}O_3$ oxides via single-source alkoxide precursors and semi-alkoxide routes. *Sol–Gel Sci Technol* 2000;**17**:145–58.
18. Nishio K, Tsuchiya T. Sol–gel processing of thin films with metal salts. In: Kozuka H, Sakka S, editors. *Handbook of sol–gel science and technology, processing characterization and applications. Applications of sol–gel technology*, vol. 1. Boston: Kluwer Academic Publisher; 2005. p. 59–76.
19. Prastomo N, Muto H, Sakai M, Matsuda A. Formation and stabilization of tetragonal phase in sol–gel derived ZrO_2 treated with base-hot-water. *Mater Sci Eng B* 2010;**173**:99–104.
20. Juarez RE, Lamas DG, Lascale GE, Walsoe de Reca NE. Synthesis of nanocrystalline zirconia powders for TZP ceramics by a nitrate–citrate combustion route. *J Eur Ceram Soc* 2000;**20**:133–8.
21. Li X, Wang D, Cheng G, Luo Q, An J, Wang Y. Preparation of polyaniline-modified TiO_2 nanoparticles and their photocatalytic activity under visible light illumination. *Appl Catal B: Environ* 2008;**81**:267–73.